

Exploring the Trojan Horse Method for Nuclear Fusion Data

Dominik Stajkowski^{1,}, Tzany Kokalova¹, Carl Wheldon¹, and Jack Bishop¹*

¹School of Physics and Astronomy, University of Birmingham, Edgbaston, Birmingham, B15 2TT, United Kingdom.

Abstract. The Trojan Horse Method (THM) is an indirect technique which extracts a two-body cross-section of interest from a related three-body reaction. The need for the application of the THM for obtaining fusion data is outlined, with a focus on the $^{93}\text{Nb}(\text{n}, \gamma)^{94}\text{Nb}$ cross-section. The basic features of THM are explained, with a particular focus on the quasi-free (QF) kinematics and the resulting energy relations, which provide a way to link the spectator momentum to the interaction energy of interest. The QF kinematics are then applied to the $^{93}\text{Nb}(\text{d}, \text{p}\gamma)^{94}\text{Nb}$ reaction, with some experimental considerations being outlined. A follow-up measurement to validate the THM result using the High-Flux Accelerator Driven Neutron Facility (HF-ADNeF) is proposed.

1 Introduction

To avoid future decommissioning issues associated with long-lived waste, the nuclear fusion sector aims to have experimental data on the activation cross-sections of all materials used in fusion reactors. Neutrons are of particular interest as they are unaffected by magnetic fields and are highly penetrating in matter, leading to them having a large range in possible reactors compared to other fusion products.

Deuterium-tritium fusion reactor components will experience neutron energies ranging from thermal (≈ 0.025 eV) up to ≈ 15 MeV [1]. Obtaining relevant cross-sections over such a wide energy range is a challenging task. The two easiest ways of acquiring such data are neutron time of flight (nToF) measurements, which require specialised facilities, or using neutron unfolding [2] with a white neutron source of a known energy profile. These methods require relatively uncommon facilities, making them unsuitable to meet the demand for fusion-related neutron cross-sections where many cross-sections need to be determined.

In the following sections, the main features of the Trojan Horse Method (THM) will be discussed to show that this indirect technique can be a relatively easy alternative for obtaining the much-needed data. Following is a proposed measurement of the $^{93}\text{Nb}(\text{n}, \gamma)^{94}\text{Nb}$ cross-section in the neutron energy range of interest, with relevant kinematic considerations.

Niobium-93 (the only naturally occurring isotope of Nb) was chosen, as it is used in plasma-confining superconducting magnets, which are exposed to high neutron fluxes. Activation of this component can have a large impact on decommissioning. In particular, ^{93}Nb can react with neutrons to produce radionuclides with half-lives ranging from 15 s to 2×10^4 y [3]. The longest lived of

those isotopes, ^{94}Nb produced via a (n, γ) reaction, β^- decays into ^{94}Mo ; this decay is associated with an emission of 703 keV and 871 keV γ rays [4]. Understanding the production of this radionuclide over the relevant energy range will impact the decommissioning plans of the fusion reactors, with possible implications for future fusion power plant designs.

2 About the Trojan Horse Method

THM uses a compound nucleus to generate a “proxy” beam of known energy to examine a cross-section over a large energy region using a single experimental configuration.

This approach was originally proposed by Baur to study nuclear reactions at astrophysically relevant energies [5]. The theoretical framework was developed by Typel [6, 7]. In THM, a Trojan Horse nucleus (TH), composed of two bound clusters ($s \oplus x$), interacts with the other participating nucleus, a , at an energy above the Coulomb barrier between the TH and a nuclei. The Trojan Horse reaction happens when TH and a are close enough for nuclear interaction to be dominant, eliminating the Coulomb suppression of the two-body $(a(x, \beta)b)$ reaction. The interaction proceeds such that only cluster x reacts with a , s being a spectator to the whole process. The resulting system $c = a + x$ reacting to form $c' = \beta + b$, is presented in Fig. 2.

The reaction mechanism in Fig. 2 dominates when no momentum is transferred to the spectator [7], leading to the Quasi-Free (QF) nature of the interaction. Under this condition, x is virtual and does not obey the typical energy dispersion equation, giving the reaction a Half Off the Energy Shell (HOES) nature. In practice, it is preferable to vary the magnitude of the momentum of s , p_s , around the QF value to explore a wider energy range. To ensure the HOES nature of the reaction, a cut-off in the spectator momentum (corresponding to the On the Energy Shell (OES)

*e-mail: d.stajkowski.1@pgr.bham.ac.uk

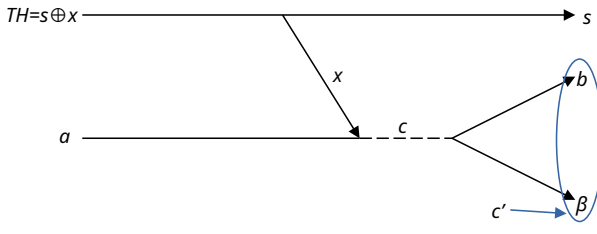


Figure 1. A pseudo-pole diagram of the *TH* reaction in which the Trojan horse (*TH*), composed of $x \oplus s$, is used to generate a "proxy beam" of species x . The particle s is the spectator to the reaction $x+a$, which results in c that decays into β and b , labelled as c' .

value) is used. This cut-off value represents the maximum momentum the spectator can have within the *TH* nucleus while remaining bound [8]:

$$p_{xs} \leq \sqrt{2\mu_{xs}B_{xs}}, \quad (1)$$

where p_{xs} is the magnitude of the relative momentum between x and s , μ_{xs} is the reduced mass of $x+s$ system, and B_{xs} is the binding energy of the two clusters in the *TH*, defined to be positive for bound systems.

There are many approaches to linking the measured three-body cross-section, associated with $TH(a, \beta b)s$ reaction, to the two-body cross-section of interest corresponding to the $x(a, \beta b)$ reaction, each depending on different approximations (see Reference [8] and references within for details). The simplest way of extracting the two-body cross-section is using the Modified Plane Wave Impulse Approximation (MPWIA). The application of this approximation requires the energy between a and *TH* to be much greater than B_{xs} [9]:

$$E_{aTH} \gg B_{xs}. \quad (2)$$

The two-body differential cross section and the three-body differential cross sections [10] are linked, using PWIA via [11]:

$$\frac{d^3\sigma_{TH(a,s\beta)b}}{dE_{b\beta}d\Omega_{b\beta}d\Omega_{sc'}} = (KF) |\Psi(p_{xs})|^2 \left. \frac{d\sigma_{a(x,\beta)b}}{d\Omega} \right|_{HOES}, \quad (3)$$

where (KF) is a kinematic factor and $|\Psi(p_{xs})|^2$ is the momentum distribution of the clusters in the *TH*. The two-body cross-section on the right-hand side of Eqn. 3 has a HOES nature and does not account for the Coulomb barrier between $a - x$, since the interaction takes place in the nuclear field. Therefore, the two-body cross-section contains mainly the nuclear part of the contribution to the cross-section of interest. Additionally, due to the use of PWIA, the HOES cross-section is missing the magnitude information, giving only the energy dependence of the nuclear part of the cross-section.

To obtain the OES two-body cross-section, the HOES cross-section from Eqn. 3 has to be scaled by a factor of:

$$\left(\frac{d\sigma_{a(x,\beta)b}}{d\Omega} \right)_l = \frac{N}{C_{ax,l}} \left. \frac{d\sigma_{a(x,\beta)b}}{d\Omega} \right|_{HOES}, \quad (4)$$

where: N is a scaling factor derived from normalising the *THM* data to a direct measurement and $C_{ax,l}$ is the Coulomb penetrability factor given by:

$$C_{ax,l} = \left(F_l^2(k_{ax}R_{ax}) + G_l^2(k_{ax}R_{ax}) \right)^{-1}, \quad (5)$$

where F_l^2 and G_l^2 are the regular and irregular Coulomb functions respectively, depending on the orbital angular momentum l between x and a , k_{xa} is the wave number corresponding to the magnitude of the relative momentum between a and x (p_{xa}), and R_{ax} is the interaction radius.

THM has been successfully used for obtaining many cross sections in the low energy region, typically for nuclear astrophysics (see Table 1 in reference [12]).

3 Quasi-Free Kinematics

As mentioned above, the condition of negligible momentum transfer to the spectator has to be met so that the two-body cross section can be extracted from the three-body reaction; this leads to x being a virtual particle that does not obey the typical energy dispersion equation, implying:

$$E_x \neq \frac{p_x^2}{2m_x}, \quad (6)$$

but x does obey momentum conservation within the QF restriction.

3.1 Momentum

Momentum conservation requires that the sum of the momenta of the products must be the same as the momentum of the beam particle \mathbf{p}_j :

$$\begin{aligned} \mathbf{p}_j &= \mathbf{p}_s + \mathbf{p}_b + \mathbf{p}_\beta \\ &= \mathbf{p}_s + \mathbf{p}_{c'}, \end{aligned} \quad (7)$$

where \mathbf{p} is the momentum vector of the particle given by the subscript which follows the convention presented in Fig. 2 with j representing the beam species (a or *TH* depending on the set up).

In the reference frame in which the *TH* is initially at rest, the momentum magnitude of the spectator, p_s , (related to p_{xs}) follows its momentum distribution in the *TH*, when PWIA is valid [13]:

$$p_s \sim |\Psi(p_s)|^2, \quad (8)$$

where for two clusters bound with no orbital angular momentum, $l = 0$, $|\Psi(p_s)|^2$ can be described via the Fourier Transform of the Hulthén function [14], given as:

$$\Psi(p_s) = \frac{1}{\pi} \sqrt{\frac{\alpha\gamma(\alpha + \gamma)}{(\alpha - \gamma)^2}} \left(\frac{1}{\alpha^2 + p_s^2} - \frac{1}{\gamma^2 + p_s^2} \right), \quad (9)$$

with parameters of $\alpha = 0.2317 \text{ fm}^{-1}$ and $\gamma = 1.202 \text{ fm}^{-1}$, for a deuteron [15].

Alternative approximations, such as the distorted-wave (DWBA) and plane-wave (PWBA) Born approximations,

can be used, leading to different spectator momentum distributions. However, within the region of interest, the difference between the possible approximations is often negligible compared with experimental uncertainties, as shown by Cognata [13], however PWIA is recommended to minimise the parameter dependency of the results.

Regardless of the approximation, the QF condition and the spectator momentum cut-off limit the kinematics of the reaction, and in the case where the TH is the beam species, this dictates the maximum deviation of s from the beam axis.

3.2 Interaction Energy

To derive the interaction energy between x and a , consider the energy conservation for the two reactions:

$$\text{Two-body: } E_{xa} = E_{\beta b} - Q_2 \\ \text{and}$$

$$\text{Three-body: } E_{aTH} + E_{CoM,i} = E_{\beta b} + E_{c's} - Q_3 + E_{CoM,f}, \quad (10)$$

where:

- E_{ij} is the energy of relative motion between i and j ,
- c' denotes the $\beta + b$ system, as seen in Fig. 2,
- $Q_2 = m_a + m_x - m_b - m_\beta = m_a + m_x - m_{c'}$ is the Q-value of the two-body reaction,
- $Q_3 = m_a + m_{TH} - m_s - m_b - m_\beta = m_a + m_{TH} - m_s - m_{c'}$ is the Q-value of the three-body reaction, and
- $E_{CoM,k}$ is the centre of mass (CoM) energy, with $k = i$ indicating the initial state with particles TH and a , and $k = f$ being the final state with particles s, β and b .

For simplicity the speed of light, c , is set to unity, making mass, momentum, and energy have the same units; hence, Q_3 can represent both the Q-value of the three-body reaction and the change in mass caused by this reaction.

Equation 10 can be rearranged to remove $E_{\beta b}$:

$$E_{xa} = E_{aTH} - E_{c's} - B_{sx} + E_{CoM,i} - E_{CoM,f}. \quad (11)$$

Using the definition of relative energy and noting that, in the lab frame, the target species, k (either TH or a), is stationary, making $p_k = 0$ MeV/c, leads to:

$$E_{aTH} = \frac{m_k}{(m_{TH} + m_a)} E_j, \quad (12)$$

where subscript j indicates the beam particle (a or TH) and subscript k indicates the target (TH or a).

Using similar logic and Eqn. 7, $E_{c's}$ can be expressed as:

$$E_{c's} = \frac{p_s^2}{2\mu_{c's}} + \frac{m_j \mu_{c's} E_j}{m_{c'}^2} - \frac{\mathbf{p}_j \cdot \mathbf{p}_s}{m_{c'}}. \quad (13)$$

Expanding the CoM terms and rearranging gives:

$$E_{CoM,i} - E_{CoM,f} = \frac{-Q_3 m_j}{(m_a + m_{TH})(m_s + m_{c'})} E_j \\ = \frac{-Q_3 \mu_{aTH} \mu_{c's}}{m_k m_s m_{c'}} E_j. \quad (14)$$

Combining Eqn. 11, 12, 13 and 14 and rearranging:

$$E_{xa} = \left(\frac{m_k}{(m_{TH} + m_a)} - \frac{m_j \mu_{c's}}{m_{c'}^2} - \frac{Q_3 \mu_{aTH} \mu_{c's}}{m_k m_s m_{c'}} \right) E_j \\ - B_{sx} - \frac{p_s^2}{2\mu_{c's}} + \frac{\mathbf{p}_j \cdot \mathbf{p}_s}{m_{c'}}. \quad (15)$$

Equation 15 outlines the two main features of THM: the energy drop from the beam energy, E_j , to the interaction energy, E_{xa} , and the energy range spanned for a given E_j due to the magnitude and direction of \mathbf{p}_s . While the most probable difference between the beam and the proxy beam, corresponding to $p_s = 0$ MeV/c, can be obtained only from the masses of the particles involved and the beam energy, the exact value of E_{xa} also depends on the spectator momentum; hence in THM investigation knowing this quantity is vital; this can be either achieved by detecting the spectator directly and tagging it to the decay channel of interest or by carrying out an experiment in which all particles originating from the compound system are detected such that the spectator momentum can be reconstructed from the detected particles.

4 $^{93}\text{Nb}(n, \gamma)^{94}\text{Nb}$ via $^{93}\text{Nb}(d, p\gamma)^{94}\text{Nb}$

The current theoretical framework shows that THM can be used for investigating radiative capture reactions [6], although there have been no experiments using it in this capacity. Additionally, it is not clear, from theory, whether THM is applicable to neutron-induced reactions in heavier nuclei since the QF reaction is innately a peripheral process, which is not the case for a typical neutron interaction, as it interacts with the whole nucleus; hence the partial wave composition may be different for the THM and direct irradiation, leading to a different energy dependence of the cross-section. So far, THM has been used to investigate neutron-induced reactions in systems as heavy as ^{25}Mg and ^{27}Al [16], although the results are yet to be published.

To investigate the feasibility of using THM for neutron-induced reaction in heavier nuclei, the $^{93}\text{Nb}(n, \gamma)^{94}\text{Nb}$ cross-section will be investigated. As mentioned in the introduction, this process is of interest for nuclear fusion in the energy range from thermal energies up to 15 MeV. Currently, the cross-section is well known from 10 meV to 3 MeV with only two high energy data points at 14.06 MeV and 14.7 MeV. This investigation aims to apply a nuclear astrophysics tool, THM, to investigate a cross-section relevant to fusion power.

To study this cross-section at a relevant energy range it is proposed to use the $^{93}\text{Nb}(d, p\gamma)^{94}\text{Nb}$ three-body reaction to obtain the energy dependence of the $^{93}\text{Nb}(n, \gamma)^{94}\text{Nb}$ cross-section, which will be scaled to known data. In this application, the deuteron will be used as the TH, "clustered" as $p \oplus n$, where the proton is the spectator; this configuration has been used before (see reference [16] and references within). The quasi-free reaction is schematically represented in Fig. 2.

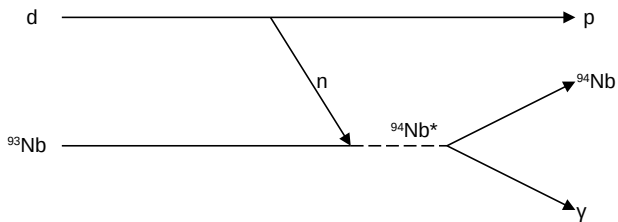


Figure 2. A pseudo-pole diagram of the three-body, $^{93}\text{Nb}(\text{d}, \text{py})^{94}\text{Nb}$, reaction, to be used to study the $^{93}\text{Nb}(\text{n}, \gamma)^{94}\text{Nb}$ cross section. The deuteron (d) being the Trojan Horse, and the proton (p) being the spectating cluster to the two-body reaction of interest.

The investigation will be carried out at the MC40 Cyclotron at the University of Birmingham [17–19], with a 20 MeV deuteron beam, which covers a CoM energy range of approximately 0–13 MeV, following Eqn. 11; this energy range overlaps with known data, allowing for cross-section normalisation in the energy range of interest.

The upper momentum limit is, from Eqn. 1, $p_{xs} \leq 45.7 \text{ MeV}/c$. This can be combined with momentum conservation of Sec. 3.1 and the interaction energy given by Eqn. 15 to carry out the kinematic calculations, the results of which are seen in Fig. 3.

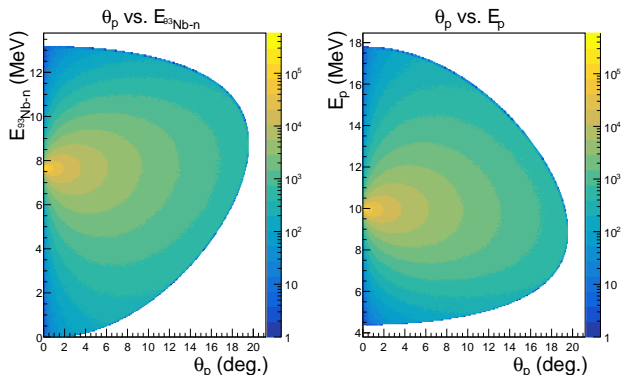


Figure 3. Kinematic plots with logarithmic z-axis, representing the reaction yield, of the relative energy between the neutron and ^{93}Nb vs the emission angle of the spectator proton (left) and the energy of the spectator proton vs its emission angle (right), both in the lab reference frame (^{93}Nb being the target).

The left plot in Fig. 3 shows the centre of mass interaction energy of ^{93}Nb and the neutron as a function of the proton emission angle in the lab frame. The highest proton emission angle for all relative energies corresponds to the maximum momentum transfer to the spectator, with the highest relative energy corresponding to emission at 180° in the centre of mass frame relative to the direction of motion of the beam species and the lowest energy corresponding to a spectator emission at 0° in the centre of mass frame.

The right plot in Fig. 3 shows the spectator proton energy and its emission angle in the lab frame. Again, the maximum angle for a given energy corresponds to the maximum momentum transfer to the spectator, the highest energy corresponding to emission at 0° in the centre of mass frame and the lowest proton energy corresponding to emission at 180° in the centre of mass frame.

Figure 3 outlines the benefits of detecting the spectator proton at small angles, as it leads to higher yields and an increase in the energy range that can be investigated. To take advantage of this, Double-sided Silicon Strip Detectors (DSSDs) will be placed as close to the beam downstream of the target as possible to detect the spectator proton. The γ rays corresponding to the population of ^{94}Nb will be detected by an array of $\text{LaBr}_3(\text{Ce})$ scintillator detectors covering $\approx 10\%$ of the solid angle to identify the desired decay channel, since the recoil ^{94}Nb cannot be detected due to its short range in Nb of $\approx 0.03 \mu\text{m}$.

5 Measurement Validation Using Direct Irradiation

To confirm the validity of THM for neutron-induced reactions in heavy nuclei, the energy dependence of the cross-section will be compared to the available data for low energies ($< 3 \text{ MeV}$); if a good agreement is seen, the THM cross-section will be scaled to match the value of the direct data, as outlined previously, to obtain the OES cross-section.

The scaled THM cross-section will be combined with the neutron energy spectrum of High Flux Accelerator-Driven Neutron Facility (HF-ADNeF) at the University of Birmingham [18, 20], to predict the ^{94}Nb activity after irradiation with high energy ($3 - 13 \text{ MeV}$) neutrons. To obtain such energies, HF-ADNeF will use a high-flux deuteron beam to produce neutrons via the $\text{d}({}^7\text{Li}, \text{n})$ reaction.

The activity expected from the scaled THM cross-section will be compared to direct irradiation values to see if the THM cross-section can accurately predict the amount of activation. If the two agree, it will validate the energy dependence of the THM cross-section. The result would also provide insight into the QF reaction mechanism used in THM, which could influence further theoretical developments regarding this method.

6 Conclusion

The basics of THM have been presented, including some key concepts and steps, such as linking the two and three-body cross-sections, in the Modified Plane Wave Impulse Approximation framework. The QF kinematics were discussed, leading to the relationship between the beam energy, the spectator momentum, and the interaction energy of the two-body reaction. A planned investigation of the $^{93}\text{Nb}(\text{n}, \gamma)^{94}\text{Nb}$ reaction via the $^{93}\text{Nb}(\text{d}, \text{py})^{94}\text{Nb}$ THM reaction has been used as an example of the restricted kinematics. Lastly, a measurement using direct neutron irradiation was outlined as a validation measurement, which

has the potential to demonstrate that THM can be used to investigate neutron-induced reactions in heavier nuclei.

References

- [1] M. Coventry, A. Krites, Measurement of D-7Li Neutron Production in Neutron Generators Using the Threshold Activation Foil Technique, Physics Procedia **90**, 85 (2017), conference on the Application of Accelerators in Research and Industry, CAARI 2016, 30 October – 4 November 2016, Ft. Worth, TX, USA. <https://doi.org/10.1016/j.phpro.2017.09.028>
- [2] M. Reginatto, Overview of spectral unfolding techniques and uncertainty estimation, in *Radiation Measurements* (2010), Vol. 45, pp. 1323–1329, ISSN 13504487
- [3] National Nuclear Data Center, information extracted from the NuDat3 database, <https://www.nndc.bnl.gov/nudat/>
- [4] D. Abriola, A. Sonzogni, Nuclear Data Sheets for $A = 94$, Nuclear Data Sheets **107**, 2423 (2006). <https://doi.org/10.1016/j.nds.2006.08.001>
- [5] G. Baur, Breakup reactions as an indirect method to investigate low-energy charged-particle reactions relevant for nuclear astrophysics, Physics Letters B **178**, 135 (1986). [10.1016/0370-2693\(86\)91483-8](https://doi.org/10.1016/0370-2693(86)91483-8)
- [6] S. Typel, H.H. Wolter, Extraction of Astrophysical Cross Sections in the Trojan-Horse Method, Few-Body Systems **29**, 75 (2000). [10.1007/s006010070010](https://doi.org/10.1007/s006010070010)
- [7] S. Typel, G. Baur, Theory of the Trojan-Horse Method, Annals of Physics **305**, 228 (2002). [10.1016/S0003-4916\(03\)00060-5](https://doi.org/10.1016/S0003-4916(03)00060-5)
- [8] A. Tumino, C.A. Bertulani, M.L. Cognata, L. Lamia, R.G. Pizzone, S. Romano, S. Typel, The Trojan Horse Method: A Nuclear Physics Tool for Astrophysics, Annual Review of Nuclear and Particle Science **71**, 345 (2021). [10.1146/annurev-nucl-102419-033642](https://doi.org/10.1146/annurev-nucl-102419-033642)
- [9] A.M. Mukhamedzhanov, A.S. Kadyrov, D.Y. Pang, Trojan horse method as an indirect approach to study resonant reactions in nuclear astrophysics, The European Physical Journal A **56**, 233 (2020). [10.1140/epja/s10050-020-00214-9](https://doi.org/10.1140/epja/s10050-020-00214-9)
- [10] S. Typel, $5\text{He}(3\text{He}, 4\text{He})4\text{He}$ as a three-body reaction via a continuum resonance in the $n+4\text{He}$ system: A tribute to Mahir S. Hussein, European Physical Journal A **56** (2020). [10.1140/epja/s10050-020-00293-8](https://doi.org/10.1140/epja/s10050-020-00293-8)
- [11] M. Jain, P. Roos, H. Pugh, H. Holmgren, The $(p, p\alpha)$ and $(\alpha, 2\alpha)$ reactions on 6Li and 7Li at 60 MeV, Nuclear Physics A **153**, 49 (1970). [10.1016/0375-9474\(70\)90756-6](https://doi.org/10.1016/0375-9474(70)90756-6)
- [12] C. Spitaleri, Trojan horse technique to measure nuclear astrophysics rearrangement reactions, Journal of Physics: Conference Series **420** (2013). [10.1088/1742-6596/420/1/012137](https://doi.org/10.1088/1742-6596/420/1/012137)
- [13] M.L. Cognata, C. Spitaleri, A. Mukhamedzhanov, V. Goldberg, B. Irgaziev, L. Lamia, R.G. Pizzone, M.L. Sergi, R.E. Tribble, DWBA momentum distribution and its effect on THM, Nuclear Physics A **834**, 658c (2010). [10.1016/j.nuclphysa.2010.01.116](https://doi.org/10.1016/j.nuclphysa.2010.01.116)
- [14] A. Tumino, C. Spitaleri, A. Mukhamedzhanov, G.G. Rapisarda, L. Campajola, S. Cherubini, V. Crucillá, Z. Elekes, Z. Fülöp, L. Gialanella et al., Off-energy-shell p-p scattering at sub-Coulomb energies via the Trojan horse method, Physical Review C **78**, 064001 (2008). [10.1103/PhysRevC.78.064001](https://doi.org/10.1103/PhysRevC.78.064001)
- [15] M. Zadro, D. Miljanic, C. Spitaleri, G. Calvi, M. Lattuada, F. Riggi, Excitation function of the quasifree contribution in the $H(Li, \alpha\alpha)n$ reaction at $E_0=28-48$ MeV, **40** (1989). <https://doi.org/10.1103/PhysRevC.40.181>
- [16] R. Spartá, C. Spitaleri, L. Lamia, G.L. Guardo, S. Cherubini, M. Gulino, M.L. Cognata, R.G. Pizzone, G.G. Rapisarda, S. Romano et al., Neutron-induced reactions investigated via the Trojan Horse Method, Journal of Physics: Conference Series **1308** (2019). [10.1088/1742-6596/1308/1/012022](https://doi.org/10.1088/1742-6596/1308/1/012022)
- [17] D. Parker, C. Wheldon, The Birmingham MC40 Cyclotron Facility, Nuclear Physics News **28**, 15 (2018). [10.1080/10619127.2018.1463021](https://doi.org/10.1080/10619127.2018.1463021)
- [18] C. Wheldon, Position sensitive detector applications in nuclear physics and nuclear industry, Journal of Instrumentation **17** (2022). [10.1088/1748-0221/17/10/C10010](https://doi.org/10.1088/1748-0221/17/10/C10010)
- [19] University of Birmingham, MC40 Cyclotron Facility, <https://www.birmingham.ac.uk/research/activity/nuclear/about-us/facilities/mc40-cyclotron-facility>
- [20] University of Birmingham, High Flux Accelerator-Driven Neutron Facility - The Birmingham Centre for Nuclear Education and Research, <https://www.birmingham.ac.uk/research/activity/nuclear/about-us/facilities/high-flux-neutron-facility>